Synthesis, Spectroscopy, and Electrochemical Studies of Binuclear Tris-Bipyridine Ruthenium(II) Complexes with Oligothiophene Bridges

Ted M. Pappenfus and Kent R. Mann*

Department of Chemistry, University of Minnesota, Minneapolis, Minnesota 55455

Received May 24, 2001

A new series of bipyridine-capped oligothiophene ligands and their binuclear Ru(II) complexes of the general formula $[(bpy)_2Ru\text{-}bpy(th)_x bpy\text{-}Ru(bpy)_2]^{4+}$ (where bpy = 2,2′-bipyridyl, th = 2,5-thienyl, and x = 1, 3, or 6) has been synthesized. Comparison of the bipyridine-capped oligothiophenes to the corresponding uncapped oligomers shows that there is coupling of the bipyridine to the oligothiophene-conjugated π-system. Each of the bipyridine-capped ligands reduces at a bipyridine cap at potentials less negative than those of free bipyridine. The λ_{max} values of the lowest $\pi-\pi^*$ transition increase and the E_{pa} values for the first oxidation decrease with an increase in the number of thiophene rings in the bridge. The increase in the number of thiophene rings also leads to more accessible oxidation states, up to four for the $x = 6$ compound. Upon complexation of the ligands with the $(bpy)_2Ru^{2+}$ moiety, the electronic spectra of the complexes show a significant redshift in comparison to the spectra of $Ru(bpy)_3^{2+}$, the oligothiophene-based oxidation(s) shifts to more positive potentials, and new oxidation and reduction processes are also observed. A single concurrent Ru(II/III) oxidation process is observed in all cases at about the same potential (E_{ave}^0 = 1.32 V (acetonitrile solution)) as is observed in the parent complex $Ru(bpy)_3^{2+}$, suggesting that the couples are not strongly coupled. The series of complexes shows a unique range of ligand-based oxidation processes with respect to the position of the Ru(II/III) redox process. In the case of $x = 1$, no ligand-based oxidation process is observed; for $x = 3$, the first oligothiophene oxidation occurs at potentials less positive than those of the Ru(II/III) redox process, and for $x = 6$, two oligothiophene oxidations are less positive than the Ru(II/III) redox process. A series of bpy reduction processes that are similar to those observed for $Ru(bpy)_3^{2+}$ also occurs. The $x = 1$ compound shows two, one-electron reductions and then two, two-electron reductions; the $x = 3$ and $x = 6$ compounds show three, two-electron reduction processes. The first reductions occur at the capping bipyridines of the bridging ligand in all three complexes, and subsequent reductions occur at the ancillary bipyridine ligands in a stepwise fashion.

Introduction

The synthesis and study of binuclear ruthenium(II) and osmium(II) polypyridyl complexes with unique redox and photophysical properties[1−11]continue to be an active area of research. Many ligands containing two bipyridine units connected by various bridges have been reported.[12] In general, these ligands are not easy to oxidize and their subsequent complexes exhibit oxidations due only to the M(III)/M(II) redox couple. Only a few examples exist where the bridging ligand oxidizes before or after the metal centers.[13−17] The synthesis of binuclear complexes with redox-active bridging ligands introduces the potential for enhanced metal−metal coupling[9,10] and properties such as vectorial electron transfer.[11]

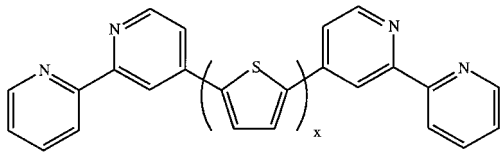

Our previous work[18−20] suggested that a series of bis-bipyridyl ligands of the general structure above could give complexes with potentially interesting redox properties.

The oligothiophene bridge introduces an attractive method of tuning the redox and electronic properties of the ligand

(1) Villahermosa, R. M.; Kuciauskas, D.; Mayo, E. I.; Lewis, N. S.; Winkler, J. R.; Gray, H. B. 221st National Meeting of the American Chemical Society; San Diego, CA, April 1−5, 2001; INOR-144.
(2) Mosher, P. J.; Yap, G. P. A.; Crutchley, R. J. *Inorg. Chem.* **2001**, *40*, 1189−1195.
(3) Juris, A.; Prodi, L.; Harriman, A.; Ziessel, R.; Hissler, M.; El-ghayoury, A.; Wu, F.; Riesgo, E.; Thummel, R. P. *Inorg. Chem.* **2000**, *39*, 3590−3589.
(4) Paul, P.; Tyagi, B.; Bilakhiya, A. K.; Dastidar, P.; Suresh, E. *Inorg. Chem.* **2000**, *39*, 14−22.
(5) El-ghayoury, A.; Harriman, A.; Khatyr, A.; Ziessel, R. *Angew. Chem., Int. Ed.* **2000**, *39*, 185−189.
(6) Barigelletti, F.; Flamigni, L. *Chem. Soc. Rev.* **2000**, *29*, 1−12.
(7) El-ghayoury, A.; Harriman, A.; Khatyr, A.; Ziessel, R. *J. Phys. Chem. A* **2000**, *104*, 1512−1523.
(8) O'Reilly, F. M.; Kelly, J. M. *J. Phys. Chem. B* **2000**, *104*, 7206−7213.
(9) Chiorboli, C.; Bignozzi, C. A.; Scandola, F.; Ishow, E.; Gourdon, A.; Launay, J.-P. *Inorg. Chem.* **1999**, *38*, 2402−2410.
(10) Ishow, E.; Gourdon, A.; Launay, J.-P.; Chiorboli, C.; Scandola, F. *Inorg. Chem.* **1999**, *38*, 1504−1510.
(11) Schlicke, B.; Belser, P.; Cola, L. D.; Sabbioni, E.; Balzani, V. *J. Am. Chem. Soc.* **1999**, *121*, 4207−4214.
(12) For a recent review of bridging bipyridine ligands, see: Kaes, C.; Katz, A.; Hosseini, M. W. *Chem. Rev.* **2000**, *100*, 3553−3590.
(13) Das, A.; Shukla, A. D. *Polyhedron* **2000**, *19*, 2605−2611.
(14) Keyes, T. E.; Forster, R. J.; Jayaweera, P. M.; Coates, C. G.; McGarvey, J. J.; Vos, J. *Inorg. Chem.* **1998**, *37*, 5925−5932.
(15) Paw, W.; Connick, W. B.; Eisenberg, R. *Inorg. Chem.* **1998**, *37*, 3919−3926.
(16) Hartl, F.; Snoeck, T. L.; Stufkens, D. J.; Lever, A. B. P. *Inorg. Chem.* **1995**, *34*, 3887.
(17) Joulie, L. F.; Schatz, E.; Ward, M. D.; Weber, F.; Yellowlees, L. J. *J. Chem. Soc., Dalton Trans.* **1994**, 799−804.

10.1021/ic010549e CCC: $20.00
Published on Web 10/24/2001

Table 1. Electronic Spectral Data

compd	λ_{max} (nm) (ϵ (10^4 M^{-1} cm^{-1}))[a]
thiophene	243[b]
1, Bu_2Tth	336
2, Bu_4Sth	408
7, bpy(th)bpy	240 (2.7), 282 (2.7), 338 (3.4)
8, bpy(Bu_2Tth)bpy	244 (3.7), 282 (3.9), 398 (3.9)
9, bpy(Bu_4Sth)bpy	240 (4.1), 280 (3.8), 431 (5.7)
10, $[(bpy)_2$-Ru-**7**-Ru-$(bpy)_2]^{4+}$	246 (5.5), 289 (15), 339 (3.1), 432 sh (3.4), 479 (4.8)
11, $[(bpy)_2$-Ru-**8**-Ru-$(bpy)_2]^{4+}$	247 (6.9), 290 (16), 475 (6.8)
12, $[(bpy)_2$-Ru-**9**-Ru-$(bpy)_2]^{4+}$	245 (7.1), 289 (15), 473 (7.8)
$[Ru(bpy)_3]^{2+}$	452[c] (1.6)

[a] Dichloromethane solutions. Reported values of ϵ are not corrected for overlap with other absorption bands. [b] Value from ref 45. [c] Value from ref 46.

relative to the metal by changing the oligomer length.[21,22] In addition, thiophene oligomers have been shown to form stable molecules in oxidized states[18−28] that can also π-stack in solution or in the solid state. Intermolecular association offers the possibility of producing supramolecular species with technological implications.[29]

A few brief experimental studies have been reported with oligothiophene-bridged complexes. For example, ruthenium and other metal polypyridyl complexes[30−33] with thiophene and related oligomer substituents have been anodically polymerized. Recently, a binuclear ruthenium terpyridine complex with a thiophene spacer was shown to be luminescent.[34] In a third example, a binuclear ruthenium complex with a thiophene-containing "photochromic bridge" displayed unique electron-transfer processes.[35]

We now report convenient preparations, electronic spectral measurements, and preliminary electrochemical studies of bis-bipyridine ligands with oligothiophene bridges and their binuclear ruthenium(II) complexes.

Experimental Section

Safety Note. *CAUTION!* Appropriate safety measures should be followed when using the organolithium and organostannane reagents described here due to their pyrophoric and toxic natures, respectively.

General Considerations. Unless otherwise noted, all synthetic procedures were carried out under an inert Ar atmosphere with oven-dried glassware. Toluene and tetrahydrofuran were distilled (under N_2) from Na/benzophenone and dichloromethane from P_2O_5. 3′,4′-Dibutyl-2,2′:5′,2″-terthiophene (**1**),[36] 2,5-bis(trimethylstannyl)thiophene (**4**),[37] 4-bromo-2,2′-bipyridine,[38] and *cis*-$Ru(bpy)_2Cl_2 \cdot 2H_2O$[39] were prepared as reported earlier. $Fe(acac)_3$ and $Pd(PPh_3)_2Cl_2$ were purchased from Strem Chemicals, Inc., and used as received. Tetrabutylammonium hexafluorophosphate ($TBAPF_6$) was purchased from Southwestern Analytical Chemicals and dried prior to use. Trimethyltin chloride (1.0 M in THF) and *n*-butyllithium (2.5 M in hexanes) were purchased from Aldrich. ^1H and ^{13}C NMR spectra were recorded on a Varian VXR-300 or VXR-500 MHz instrument. Chemical shifts are reported in parts per million (ppm) and referenced to the residual chloroform peak (7.26 ppm), dichloromethane peak (5.32 ppm), or acetonitrile peak (1.95 ppm). UV−vis spectra were recorded in nondegassed solutions at room temperature with a computer-interfaced Cary-17 spectrometer. Extinction coefficients were calculated from the experimentally determined absorbances using Beer's law. Electrochemical experiments were performed with a BAS 100B electrochemical analyzer using methods previously described.[20] Potentials are reported vs aqueous Ag/AgCl and are not corrected for the junction potential. The $E^{o\prime}$ values for the ferrocenium/ferrocene couple for concentrations similar to those used in this study were +0.40 and +0.46 V for acetonitrile and dichloromethane solutions, respectively, at a glassy carbon electrode. Osteryoung square wave voltammograms were obtained at a frequency of 15 Hz, a step potential of 4 mV, and an amplitude of 25 mV. The relative *n* values reported in Table 2 were determined by numerical integration of the square wave voltammograms.

3′,4′,3‴,4‴-Tetrabutyl-2,2′:5′,2″:5″,2‴:5‴,2⁗:5⁗,2⁗′:5⁗′,2⁗′′-sexithiophene (2). To a dry 500 mL round-bottom flask equipped with an Ar inlet, **1** (7.3 g, 20.2 mmol), and 110 mL of THF was added *n*-butyllithium (8.1 mL, 20.3 mmol) at −78 °C over 35 min. The reaction mixture was stirred at −78 °C for an additional 30 min and then warmed to 0 °C before it was transferred via a cannula to a solution of $Fe(acac)_3$ (7.15 g, 20.2 mmol) in 30 mL of THF. After being refluxed for 19 h, the reaction mixture was allowed to cool to room temperature. The red precipitate was filtered and washed with dichloromethane. The filtrates were concentrated to provide a red solid. The crude solid was adsorbed on silica gel (60−200 mesh) and purified via column chromatography (100% hexanes, followed by 10, 20, and 25% dichloromethane in hexanes) to yield 3.24 g (44.5%) of **2** as a yellow-orange solid. ^1H NMR (500 MHz, CD_2Cl_2): δ 7.35 (dd, 2H, J = 5.5,

(18) (a) Hill, M. G.; Penneau, J. F.; Zinger, B.; Mann, K. R.; Miller, L. L. *Chem. Mater.* **1992**, *4*, 1106−1113. (b) Zinger, B.; Mann, K. R.; Hill, M. G.; Miller, L. L. *Chem. Mater.* **1992**, *4*, 1113−1118. (c) Hill, M. G.; Mann, K. R.; Miller, L. L.; Penneau, J.-F. *J. Am. Chem. Soc.* **1992**, *114*, 2728−2730.

(19) (a) Graf, D. D.; Campbell, J. P.; Mann, K. R.; Miller, L. L. *J. Am. Chem. Soc.* **1996**, *118*, 5480−5481. (b) Graf, D. D.; Duan, R. G.; Campbell, J. P.; Miller, L. L.; Mann, K. R. *J. Am. Chem. Soc.* **1997**, *119*, 5888−5899.

(20) (a) Graf, D. D.; Mann, K. R. *Inorg. Chem.* **1997**, *36*, 150−157. (b) Graf, D. D.; Mann, K. R. *Inorg. Chem.* **1997**, *36*, 141−149. (c) Graf, D. D.; Mann, K. R. *Inorg. Chem.* **1995**, *34*, 1562−1575.

(21) (a) Miller, L. L.; Yu, Y. *J. Org. Chem.* **1995**, *60*, 6813−6819. (b) Yu, Y.; Gunic, E.; Zinger, B.; Miller, L. L. *J. Am. Chem. Soc.* **1996**, *118*, 1013−1018.

(22) Guay, J.; Kasai, P.; Diaz, A.; Wu, R.; Tour, J. M.; Dao, L. H. *Chem. Mater.* **1992**, *4*, 1097−1105.

(23) (a) Bauerle, P.; Segelbacher, U.; Maier, A.; Mehring, M. *J. Am. Chem. Soc.* **1993**, *115*, 10217−10223. (b) Segelbacher, U.; Sariciftci, N. S.; Grupp, A.; Bauerle, P.; Mehring, M. *Synth. Met.* **1993**, *55*−*57*, 4728−4733.

(24) (a) Hotta, A.; Waragi, K. *J. Phys. Chem.* **1993**, *97*, 7427−7434. (b) Tanaka, K.; Matsuura, Y.; Oshima, Y.; Yamabe, T.; Hotta, S. *Synth. Met.* **1994**, *66*, 295−298.

(25) (a) Zotti, G.; Schiavon, G.; Berlin, A.; Pagani, G. *Chem. Mater.* **1993**, *5*, 430−436. (b) Zotti, G.; Schiavon, G.; Berlin, A.; Pagani, G. *Chem. Mater.* **1993**, *5*, 620−624. (c) Zotti, G.; Berlin, G.; Pagani, G.; Schiavon, G.; Zecchin, S. *Adv. Mater.* **1994**, *6*, 231−233.

(26) (a) Hapiot, P.; Audebert, P.; Monnier, K.; Pernaut, J.-M.; Garcia, P. *Chem. Mater.* **1994**, *6*, 1549−1555. (b) Audebert, P.; Garcia, P.; Hapiot, P.; Monnier, K.; Pernaut, J.-M. *J. Chim. Phys. Phys.*−*Chim. Biol.* **1995**, *92*, 827−830. (c) Audebert, P.; Hapiot, P.; Pernaut, J.-M.; Garcia, P. *J. Electroanal. Chem.* **1993**, *361*, 283−287.

(27) Nessakh, B.; Horowitz, G.; Garnier, F.; Deloffre, F.; Srivastava, P.; Yassar, A. *J. Electroanal. Chem.* **1995**, *399*, 97−103.

(28) van Haare, J. A. E. H.; Havinga, E. E.; van Dongen, J. L. J.; Janseen, R. A. J.; Cornil, J.; Bedas, J.-L. *Chem. Eur. J.* **1998**, *4*, 1509−1522.

(29) (a) Kunugi, Y.; Mann, K. R.; Miller, L. L.; Exstrom, C. L. *J. Am. Chem. Soc.* **1998**, *120*, 589−590. (b) Kunugi, Y.; Miller, L. L.; Mann, K. R.; Pomije, M. K. *Chem. Mater.* **1998**, *10*, 1487−1489.

(30) Walters, K. A.; Trouillet, L.; Guillerez, S.; Schanze, K. S. *Inorg. Chem.* **2000**, *39*, 5496−5509.

(31) Trouillet, L.; De Nicola, A.; Guillerez, S. *Chem. Mater.* **2000**, *12*, 1611−1621.

(32) Zotti, G.; Zecchin, S.; Schiavon, G.; Berlin, A.; Penso, M. *Chem. Mater.* **1999**, *11*, 3342−3351.

(33) Zhu, S. S.; Kingsborough, R. P.; Swager, T. M. *J. Mater. Chem.* **1999**, *9*, 2123−2131.

(34) Constable, E. C.; Housecraft, C. E.; Schofield, E. R.; Encinas, S.; Armaroli, N.; Barigelletti, F.; Flamigni, L.; Figgemeier, E.; Vos, J. G. *Chem. Commun.* **1999**, 869−870.

(35) Fraysse, S.; Coudret, C.; Launay, J.-P. *Eur. J. Inorg. Chem.* **2000**, 1581−1590.

(36) Wang, C.; Benz, M. E.; LeGoff, E.; Schinder, J. L.; Allbritton-Thomas, J.; Kannewurf, C. R.; Kanatzidis, M. G. *Chem. Mater.* **1994**, *6*, 401.

(37) Seitz, D. E.; Lee, S. H.; Hanson, R. N.; Bottaro, J. C. *Synth. Commun.* **1983**, *13*, 121−128.

(38) Mizuno, T.; Takeuchi, M.; Hamachi, I.; Nakashima, K.; Shinkai, S. *J. Chem. Soc., Perkin Trans. 2* **1998**, 2281−2288.

(39) Sullivan, B. P.; Salmon, D. J.; Meyer, T. J. *Inorg. Chem.* **1978**, *17*, 3334.

Table 2. Electrochemical Data for Ligands and Complexes[a]

compd	bridging ligand oxidations	Ru(II/III)	bridging ligand reductions	ancillary bpy reductions
7, bpy(th)bpy	1.76[b]		−1.75	
8, bpy(Bu_2Tth)bpy	1.10, 1.48[b]		−1.78[c]	
9, bpy(Bu_4Sth)bpy	0.79, 1.02, 1.73,[b] 1.99[b]		−1.82[c]	
10, [(bpy)2-Ru-**7**-Ru-$(bpy)_2$]$^{4+}$	[d]	1.37[c] (**n** = 2) (1.29) (**n** = 2)	−1.05, −1.26 (−1.11), (−1.30)[c]	−1.51, −1.84[c] (**n** = 2) (−1.50),[c] (−1.85)[c] (**n** = 2)
11, [$(bpy)_2$-Ru-**8**-Ru-$(bpy)_2$]$^{4+}$	1.17, 1.77[b] (1.15), (1.73)[b]	1.41[c] (**n** = 2) (1.33) (**n** = 2)	−1.22 (**n** = 2) (−1.27) (**n** = 2)	−1.51, −1.79[c] (**n** = 2) (−1.45),[c] (−1.84)[c] (**n** = 2)
12, [$(bpy)_2$-Ru-**9**-Ru-$(bpy)_2$]$^{4+}$	0.86, 1.03, 1.80,[c] 2.04[b] (0.87), (0.99), (1.79), (1.99)[c]	1.41[c] (**n** = 2) (1.33) (**n** = 2)	−1.24 (**n** = 2) (−1.27) (**n** = 2)	−1.52, −1.80[c] (**n** = 2) (−1.41),[c] (−1.87)[c] (**n** = 2)
$[Ru(bpy)_3]^{2+}$		(1.29)	(−1.35)[e]	(−1.54), (−1.79)[c]

[a] Measured at room temperature with a scan rate of 100 mV/s in 0.1 M $TBA^+PF_6^-$ in dichloromethane; values in parentheses are measured in acetonitrile; $n = 1$ except as noted in bold. All values are $E^{\circ\prime}$ values, unless otherwise noted. [b] Irreversible process, E_{pa} value given. [c] Value obtained from the square wave voltammogram. [d] Not observed to the solvent limit. [e] Ancillary bpy reduction.

1.0 Hz), 7.16 (d, 4H, J = 3.5 Hz), 7.08 (m, 4H), 2.74 (m, 8H), 1.50 (m, 16H), 0.97 (m, 12H). HRFABMS: calcd for $C_{40}H_{46}S_6$, 718.1924; found, 718.1940.

3′,4′,3‴,4‴,3⁗,4⁗-Hexabutyl-2,2′:5′,2″:5″,2‴:5‴,2⁗:5⁗,2⁗′:5⁗′,2⁗′′:5⁗′′,2⁗′′′:5⁗′′′,2⁗′′′′-novithiophene (3). Later fractions from the column purification of compound **2** yielded 0.79 g of **3** as an orange solid. ^{1}H NMR (500 MHz, CD_2Cl_2): δ 7.35 (dd, 2H, J = 5.0, 1.0 Hz), 7.17 (m, 6H), 7.09 (m, 6H), 2.73 (m, 12H), 1.51 (m, 24H), 0.98 (m, 18H). HRFABMS: calcd for $C_{60}H_{68}S_9$, 1076.2807; found, 1076.2703.

3′,4′-Dibutyl-5,5″-bis(trimethylstannyl)-2,2′:5′,2″-terthiophene (5). To a dry 100 mL Schlenk flask containing **1** (0.88 g, 2.43 mmol) and 15 mL of THF was added *n*-butyllithium (1.98 mL, 5.10 mmol) at −78 °C over 15 min. The solution became more orange as the *n*-BuLi was added. The reaction mixture was warmed to 0 °C and allowed to stir for 0.5 h, resulting in the formation of a yellow precipitate. The suspension was then cooled to −78 °C, and a solution of trimethyltin chloride in THF (5.1 mL, 5.1 mmol) was added dropwise. The precipitate reacted slowly and gave a yellow-orange solution, which was then warmed to room temperature and allowed to stir for 45 min. The reaction mixture was poured into hexane (50 mL), washed with water, and dried with $MgSO_4$. The solvents were removed to provide 1.57 g (94%) of **5** as a viscous yellow-orange oil. ^{1}H NMR (300 MHz, $CDCl_3$): δ 7.24 (d, 2H, J = 3.3 Hz), 7.13 (d, 2H, J = 3.3 Hz), 2.71 (t, 4H), 1.55 (m, 4H), 1.44 (m, 4H), 0.96 (t, 6H), 0.38 (s, 18H). HRFABMS: calcd for $C_{26}H_{40}S_3Sn_2$, 688.0336; found, 688.0369.

3′,4′,3‴,4‴-Tetrabutyl-5,5⁗-bis(trimethylstannyl)-2,2′:5′,2″:5″,2‴:5‴,2⁗:5⁗,2⁗′-sexithiophene (6). Compound **6** was prepared from 0.49 g (0.67 mmol) of **2**, *n*-butyllithium (0.55 mL, 1.42 mmol), and trimethyltin chloride solution (1.42 mL, 1.42 mmol) using the general procedure described for the synthesis of **5** to provide 0.71 g (100%) of **6** as a thick red-orange oil. ^{1}H NMR (300 MHz, $CDCl_3$): δ 7.26 (d, 2H, J = 3.3 Hz), 7.14 (d, 2H, 3.6 Hz), 7.14 (d, 2H, J = 3.9 Hz), 7.05 (d, 2H, J = 3.9 Hz), 2.54 (m, 8H), 1.55 (m, 8H), 1.45 (m, 8H), 0.97 (m, 12H), 0.40 (s, 18H). MS (MALDI-TOF): calcd for $C_{46}H_{62}S_6Sn_2$ [M+], 1044.1; found, 1043.9.

2,5-Bis(4-2,2′-dipyridyl)-thiophene (7). To a 100 mL Schlenk flask equipped with a condenser were added **4** (1.00 g, 2.44 mmol), 4-bromo-2,2′-bipyridine (1.29 g, 5.49 mmol), and $Pd(PPh_3)_2Cl_2$ (86 mg, 0.12 mmol). The system was evacuated and backfilled with argon three times. Toluene (15 mL) was added, and the system was again evacuated and backfilled with argon three times. The reaction vessel was continually purged with argon and was heated to 110 °C for 24 h. The reaction mixture was cooled to 0 °C, and the yellow solid was filtered and washed first with cold toluene (2 × 5 mL), pentane (3 × 5 mL), and finally methanol (2 × 5 mL) to yield 0.68 g (70%) of **7** as a light-yellow solid. ^{1}H NMR (300 MHz, CD_2Cl_2): δ 8.74 (dd, 2H, J = 1.8, 0.6 Hz), 8.72 (ddd, 2H, J = 4.8, 1.8, 0.9 Hz), 8.69 (dd, 2H, J = 5.1, 0.9 Hz), 8.47 (ddd, 2H, J = 8.1, 1.2, 0.9 Hz), 7.86 (ddd, 2H, J = 8.0, 7.5, 1.8 Hz), 7.73 (s, 2H), 7.58 (dd, 2H, J = 5.3, 2.1 Hz), 7.37 (ddd, 2H, J = 7.5, 4.7, 1.5 Hz). HRMS (EI): calcd for $C_{24}H_{16}N_4S$, 392.1096; found, 392.1095.

3′,4′-Dibutyl-5,5″-bis(4-2,2′-dipyridyl)-2,2′:5′,2″-terthiophene (8). Compound **8** was prepared from 1.57 g (2.28 mmol) of **5**, 4-bromo-2,2′-bipyridine (1.21 g, 5.10 mmol), and $Pd(PPh_3)_2Cl_2$ (80 mg, 0.11 mmol) using the general procedure described for the synthesis of **7**. After being heated to 110 °C for 40 h, the reaction mixture was filtered, and the filtrates were concentrated. The crude mixture was purified further by column chromatography (silica gel) using 100% chloroform followed by 5% methanol in chloroform to provide 0.97 g (63%) of **8** as an orange solid. ^{1}H NMR (300 MHz, CD_2Cl_2): δ 8.71 (ddd, 2H, J = 4.7, 1.7, 0.9 Hz), 8.68 (dd, 2H, J = 2.1, 0.9 Hz), 8.65 (dd, 2H, J = 5.1, 0.6 Hz), 8.46 (ddd, 2H, J = 7.8, 2.1, 0.9 Hz), 7.85 (ddd, 2H, J = 7.8, 7.8, 1.8 Hz), 7.65 (d, 2H, J = 3.9 Hz), 7.52 (dd, 2H, J = 5.3, 2.1 Hz), 7.36 (ddd, 2H, J = 7.5, 4.7, 1.2 Hz), 7.24 (d, 2H, J = 3.9 Hz), 2.82 (t, 4H), 1.56 (m, 8H), 0.99 (t, 6H). HRFABMS: calcd for $C_{40}H_{36}N_4S_3$, 669.2180; found, 669.2224.

3′,4′,3‴,4‴-Tetrabutyl-5,5⁗-bis(4-2,2′-dipyridyl)-2,2′:5′,2″:5″,2‴:5‴,2⁗:5⁗,2⁗′-sexithiophene (9). Compound **9** was prepared from 0.71 g (0.68 mmol) of **6**, 4-bromo-2,2′-bipyridine (0.36 g, 1.52 mmol), and $Pd(PPh_3)_2Cl_2$ (24 mg, 0.034 mmol) using the general procedure described for the synthesis of **7**. After being heated to 110 °C for 40 h, the reaction mixture was filtered, and the filtrates were precipitated with pentane. The resulting solid was washed with pentane, methanol, and pentane again to provide 0.45 g (65%) of **9** as a deep red solid. ^{1}H NMR (300 MHz, CD_2Cl_2): δ 8.71 (ddd, 2H, J = 4.7, 1.7, 0.9 Hz), 8.68 (dd, 2H, J = 2.1, 0.9 Hz), 8.64 (dd, 2H, J = 5.1, 0.6 Hz), 8.46 (ddd, 2H, J = 8.0, 1.2, 0.9 Hz), 7.85 (ddd, 2H, J = 7.8, 7.8, 1.8 Hz), 7.64 (d, 2H, J = 3.9 Hz), 7.52 (dd, 2H, J = 5.1, 2.1 Hz), 7.36 (ddd, 2H, J = 7.5, 4.7, 1.2 Hz), 7.23 (d, 2H, J = 3.9 Hz), 7.20 (d, 2H, J = 3.6 Hz), 7.12 (d, 2H, J = 3.6 Hz), 2.80 (m, 8H), 1.55 (m, 16H), 1.00 (m, 12H). MS (MALDI-TOF): calcd for $C_{60}H_{58}N_4S_6$ [M+], 1026.3; found, 1026.3.

{[$(bpy)_2$Ru]$_2$(7)}$(PF_6)_4$ (10). A 50 mL two-necked round-bottom flask was charged with 88 mg (0.22 mmol) of **7** and 0.27 g (0.53 mmol) of *cis*-$Ru(bpy)_2Cl_2 \cdot 2H_2O$ in 10 mL of 2-methoxyethanol. The solution was purged directly with stirring for 20 min, and an argon purge was maintained thereafter. The mixture was stirred at 120 °C for 7 h; the heat was turned off, and the reaction mixture was allowed to cool to room temperature overnight. The solvent was removed under vacuum, and the resulting solid was dissolved in water and filtered to provide a deep red solution. An aqueous solution of NH_4PF_6 (0.29 g, 1.8 mmol) was added, resulting in a dark red precipitate, which was filtered and washed thoroughly with water and ether to afford 0.36 g (89%) of a dark red solid. ^{1}H NMR (300 MHz, CD_3CN): δ 8.71−8.69 (m, 4H), 8.52 (d, 8H, J = 8.1 Hz), 8.14−8.05 (m, 10H), 8.00 (s, 2H), 7.83 (ddd, 2H, J = 5.2, 1.8, 0.9 Hz), 7.78−7.72 (m, 10 H), 7.58 (dd, 2H, J = 6.0, 1.8 Hz), 7.47−7.39 (m, 10H). MS (MALDI-TOF): calcd for [M − PF_6]$^+$, 1655.1; found, 1655.0. Anal. Calcd for $C_{64}H_{48}N_{12}Ru_2SP_4F_{24}$: C, 42.72; H, 2.69; N, 9.34. Found: C, 42.96; H, 2.67; N, 9.02.

{[$(bpy)_2$Ru]$_2$(8)}$(PF_6)_4$ (11). Compound **11** was prepared from 76 mg (0.11 mmol) of **8** and 0.14 g (0.27 mmol) of *cis*-$Ru(bpy)_2Cl_2 \cdot 2H_2O$ using the general procedure described for the synthesis of **10** to provide 0.20 g (89%) of **11** as a deep red solid. ^{1}H NMR (300 MHz, CD_2Cl_2): δ 8.57 (d, 2H, J = 8.4 Hz), 8.52 (d, 2H, J = 1.8 Hz), 8.44 (d, 8H, J = 8.4 Hz), 8.12−8.03 (m, 10H), 7.86 (d, 2H, J = 4.8 Hz), 7.80 (d, 2H, J = 3.9 Hz), 7.74−7.69 (m, 8H), 7.61−7.54 (m, 4H), 7.51−7.43 (m, 10H), 7.22 (d, 2H, J = 3.9 Hz), 2.78 (t, 4H), 1.55 (m, 8H), 0.95

Scheme 1

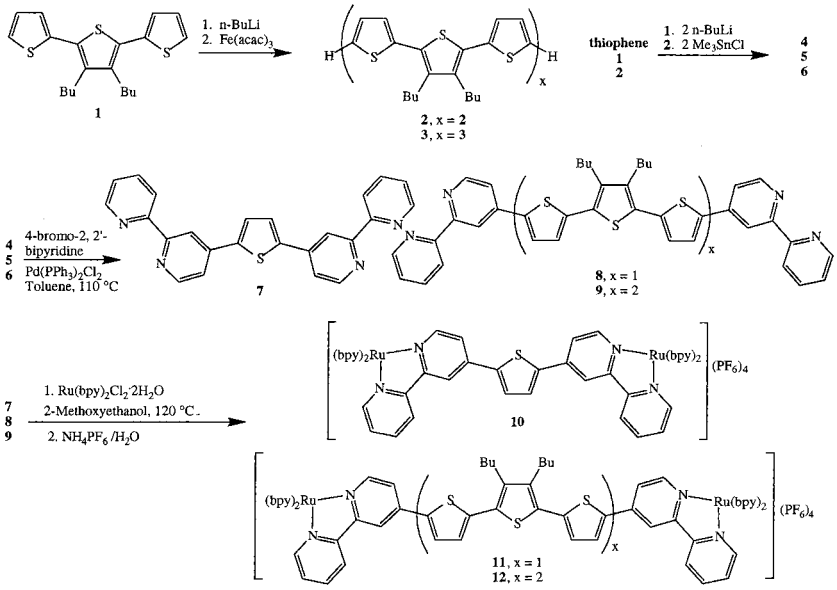

(t, 6H). MS (MALDI-TOF): calcd for $[M - PF_6]^+$, 1931.2; found, 1931.1. Anal. Calcd for $C_{88}H_{68}N_{12}Ru_2S_3P_4F_{24}$: C, 46.29; H, 3.30; N, 8.01. Found: C, 46.57; H, 3.20; N, 7.74.

{[(bpy)$_2$Ru]$_2$(9)}(PF$_6$)$_4$ (12). Compound **12** was prepared from 66 mg (0.064 mmol) of **9** and 79 mg (0.15 mmol) of *cis*-Ru(bpy)$_2$Cl$_2$·2H$_2$O using the general procedure described for the synthesis of **10** to provide 0.12 g (80%) of **12** as a deep red solid. ^{1}H NMR (300 MHz, CD_2Cl_2): δ 8.53 (d, 2H, J = 8.4 Hz), 8.49 (d, 2H, J = 1.8 Hz), 8.44 (d, 8H, J = 8.1 Hz), 8.13−8.05 (m, 10H), 7.86 (d, 2H, J = 4.8 Hz), 7.78 (d, 2H, J = 3.9 Hz), 7.74 (m, 8H), 7.61−7.54 (m, 6H), 7.51−7.44 (m, 8H), 7.27 (d, 2H, J = 3.9 Hz), 7.20 (d, 2H, J = 3.9 Hz), 7.12 (d, 2H, J = 3.9 Hz), 2.80 (m, 8H), 1.53 (m, 16H), 0.99 (t, 12H). MS (MALDI-TOF): calcd for $[M - PF_6]^+$, 2289.3; found, 2289.2. Anal. Calcd for $C_{100}H_{90}N_{12}Ru_2S_6P_4F_{24}$: C, 49.34; H, 3.73; N, 6.90. Found: C, 49.48; H, 3.83; N, 6.54.

Results and Discussion

Synthesis of Ligands and Complexes. Scheme 1 outlines the synthesis of the ligands and their {[(bpy)$_2$Ru]$_2$(bridge)}-(PF$_6$)$_4$ complexes. The ligands were prepared by standard coupling methods. The hexamer **2** was synthesized with a slight modification of a previously reported coupling procedure.[40] Homocoupling[41] of the monolithiated derivative of **1** in the presence of Fe(acac)$_3$ gave **2** as the major product. A small amount of the nonamer compound **3** was also isolated as a result of coupling with dilithiated **1**, which inadvertently formed during the lithation step. It is likely that higher oligomers are formed in this reaction mixture in even smaller amounts, but none were isolated. Bis-stannylated oligomers **5** and **6** were prepared in quantitative yields by forming dilithiated species followed by quenching with trimethyltin chloride. The bis-bipyridyl ligands were synthesized by standard Stille coupling methods[42] by adding 4-bromo-2,2′-bipyridine to the appropriate organostannane in yields that ranged between 60 and 70%.

The binuclear ruthenium complexes **10**−**12** were synthesized by adding *cis*-Ru(bpy)$_2$Cl$_2$·2H$_2$O to the appropriate ligand in 2-methoxyethanol. The use of the high-boiling solvent resulted in good yields (80−90%) with relatively short reaction times. All complexes were characterized by ^{1}H NMR spectroscopy and MALDI-TOF mass spectrometry and gave satisfactory combustion analysis results.

Electronic Spectra. The electronic spectra of the uncomplexed ligands in dichloromethane exhibit three bands (Table 1, Figure 1) that result from the independent oligothiophene and bipyridine chromophores. The band at ca. 281 nm in all three ligands is attributed to the bipyridine unit present in each of these ligands. This band is insensitive to the number of thiophene rings in the bridge. The remaining two bands are oligothiophene transitions similar to those observed previously for other oligomers: a high-energy band (245 nm) that we attribute to the $\pi-\pi^*$ local excitation of the heteronucleus,[43] which is insensitive to the number of thiophene rings, and a lower-energy band at a variable energy (338, 398, and 431 nm for x = 1, 3, and 6, respectively) that we attribute to the $\pi-\pi^*$ transition of the conjugated π-system.[44] This low-energy band shifts to a lower energy with an increase in the number of thiophene rings.[21,22]

Noteworthy is the significant effect of the bipyridine unit on the lowest-energy $\pi-\pi^*$ transition of the oligothiophene. A comparison of the lowest-energy $\pi-\pi^*$ transition of the new ligands and that of the bipyridine-free parent oligothiophenes is provided in Table 1. In every case, the bipyridine-capped ligand absorbs at significantly longer wavelengths than the uncapped parent (a 62 nm shift between the dibutylterthiophene **1** and ligand **8** and a 23 nm shift between tetrabutylsexithiophene **2** and ligand **9**). The correlation of the lowest $\pi-\pi^*$ transition energy with 1/n (where n is the number of conjugated rings) is linear with a high correlation coefficient if the n value includes the two pyridine ring capping groups. These observations suggest that the pendant pyridine ring is conjugated within the π-system of the resulting ligand.

The electronic spectra of the complexes dissolved in dichloromethane were also recorded (Table 1, Figure 1). All three complexes display one moderately intense band at ca. 246 nm, one very intense band at ca. 290 nm, and a broad, overlapping

(40) Horne, J. C.; Blanchard, G. J.; LeGoff, E. *J. Am. Chem. Soc.* **1995**, *117*, 9551−9558.
(41) For recent homocoupling procedures using Fe(acac)$_3$, see: (a) Marsella, M. J.; Carroll, P. J.; Swager, T. M. *J. Am. Chem. Soc.* **1994**, *116*, 9347. (b) Ref 21a.
(42) (a) Stille, J. K. *Pure Appl. Chem.* **1985**, *57*, 1771−1780. (b) Stille, J. K. *Angew. Chem., Int. Ed. Engl.* **1986**, *25*, 508−523. (c) Stille, J. K.; Groh, B. L. *J. Am. Chem. Soc.* **1987**, *109*, 813−817.
(43) Curtis, R. F.; Phillips, G. T. *Tetrahedron* **1967**, *23*, 4419.
(44) Murrell, J. N. *J. Chem. Soc.* **1956**, 3779.

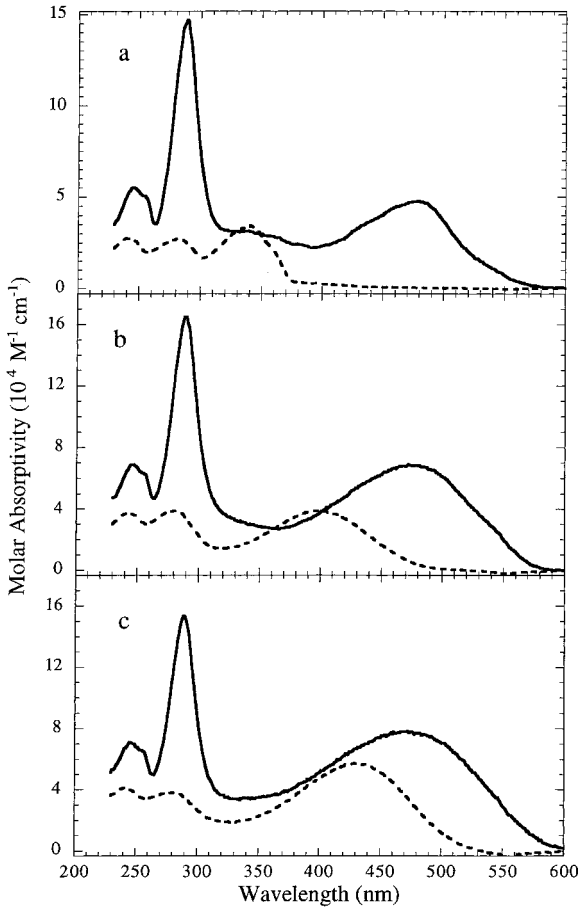

Figure 1. UV−vis spectra recorded in dichlormethane for (a) ligand **7** (- - -) and complex **10** (—), (b) ligand **8** (- - -) and complex **11** (—), and (c) ligand **9** (- - -) and complex **12** (—).

series of low-energy bands centered around 475 nm. The band at 245 nm is assigned to the thiophene localized $\pi-\pi^*$ excitation that is nearly identical to the analogous transition observed in free ligands. The very intense band at 290 nm is assigned to the $\pi-\pi^*$ transition of the bipyridine unit. It is likely that this band contains contributions from both the bridging ligand bipyridine caps and the ancillary bipyridine ligands. The high molar absorptivity of this band is consistent with our assignment.

The complicated low-energy feature in the spectrum of each complex is assigned to strongly overlapping bands due to the low-energy $\pi-\pi^*$ transition of the oligothiophene unit and the Ru(II) → bpy(π^*) MLCT transitions. The detailed assignments of the individual components of this band are difficult. One expects to observe one set of MLCT transitions (Ru → ancillary bpy(π^*)) that is insensitive to the number of thiophene rings in the bridge. Another set of Ru → bpy MLCT transitions that involve the capping bipyridine unit is expected to be somewhat more sensitive to the number of thiophene rings. Finally, the low-energy $\pi-\pi^*$ oligothiophene excitation that also depends on the number of thiophene rings is also predicted to occur in this region. These expectations are realized as there is a noticeable redshift of some components of the low-energy band in all three complexes with respect to those of the parent complex, $Ru(bpy)^{2+}$, which has a maximum absorption at 452 nm in dichloromethane[46] and some additional components that experience shifts that depend on the number of thiophene rings in the bridge. A more detailed assignment of the low-energy peaks in these complexes will require additional experiments.

Electrochemistry of the Bridging Ligands. Cyclic voltammetry studies were performed with each of the bpy(th)$_x$bpy ligands in dichloromethane (Table 2). Reductions and oxidations are observed for each of the free ligands. Reduction processes occurred at $E^{\circ\prime} = -1.75$, -1.78, and -1.82 V for ligands **7**, **8**, and **9**, respectively. Phenyl-capped oligothiophene analogues of **7**−**9** reduce at more negative potentials. Free bipyridine reduces at $E^{\circ\prime} = -2.22$ V under identical conditions. We suggest that the reduction process for **7**−**9** is centered on the bipyridine caps but is stabilized relative to bipyridine. The stabilization of the reduced forms of **7**−**9** relative to bipyridine is important in the subsequent discussion of the reduction processes of the complexes (vide infra).

At least one oxidation process was observed for each ligand. The E_{pa} value of the first oxidation process decreased with an increase in the number of thiophene rings in the bridge as expected.[21,22] By analogy to previously studied oligothiophenes, this process corresponds to the initial generation of cation radical species. The cation radical appears to be stable on the CV time scale for the terthiophene and sexithiophene ligands (**8** and **9**) but not for the single-thiophene-bridged ligand (**7**). Additionally, ligands **8** and **9** exhibit a second oxidation process that corresponds to the formation of dications; ligand **7** displays no second oxidation process out to the solvent limit. The dication formed from **9** is stable on the CV time scale, whereas the dication of **8** is not. Most remarkably, the sexithiophene-bridged ligand **9** undergoes two additional oxidation processes (generation of a trication radical and tetracation), similar to processes we have observed for the phenyl-capped sexithiophene analogue.[47] Unfortunately, these processes do not appear to generate species with high stability in the case of the bipyridyl-capped ligands.

Electrochemistry of the Complexes. Cyclic voltammetry and Osteryoung square wave voltammetry studies were performed with each of the complexes in both dichloromethane and acetonitrile (Table 2, Figures 2−4). Digital integration of the peaks in the square wave voltammetry experiments allowed relative *n* values to be determined for the processes observed for the complexes. In dichloromethane, the reduction processes of the complexes are reversible and the reduced species are soluble (Figure 2). The oxidized species generated in the anodic processes observed in this solvent are less soluble and probably precipitate on the electrode surface as indicated by the large current "spike" in all three complexes. In acetonitrile, an opposite effect is observed. In general, the reduced species become insoluble, and the oxidized species remain soluble in the more polar solvent (Figure 3). The current spikes in the acetonitrile data are no longer present when the oxidation processes are reversed but are present in the reversal of the reduction processes.

The cyclic voltammogram of the single-thiophene-bridged complex **10** in acetonitrile (shown in Figure 3a) exhibits a reversible oxidation process with $E^{\circ\prime} = 1.29$ V in agreement with the observed position of the Ru(II/III) couple of the parent complex, $Ru(bpy)_3^{2+}$, under identical conditions. This process is formally assigned to an $n = 2$ process that results from the concurrent oxidation of both Ru(II/III) redox couples. No further oxidations that could be attributed to the oxidation of the bridging ligand are observed under the experimental conditions

(45) Jung, T. S.; Kim, J. H.; Jang, E. K.; Kim, D. H.; Shim, Y.; Park, B.; Shin, S. C. *J. Organomet. Chem.* **2000**, *599*, 232−237.
(46) Durham, B.; Walsh, J. L.; Carter, C. L.; Meyer, T. J. *Inorg. Chem.* **1980**, *19*, 860−865.
(47) Pappenfus, T.; Mann, K. R. *Chem. Mater.* Submitted for publication.

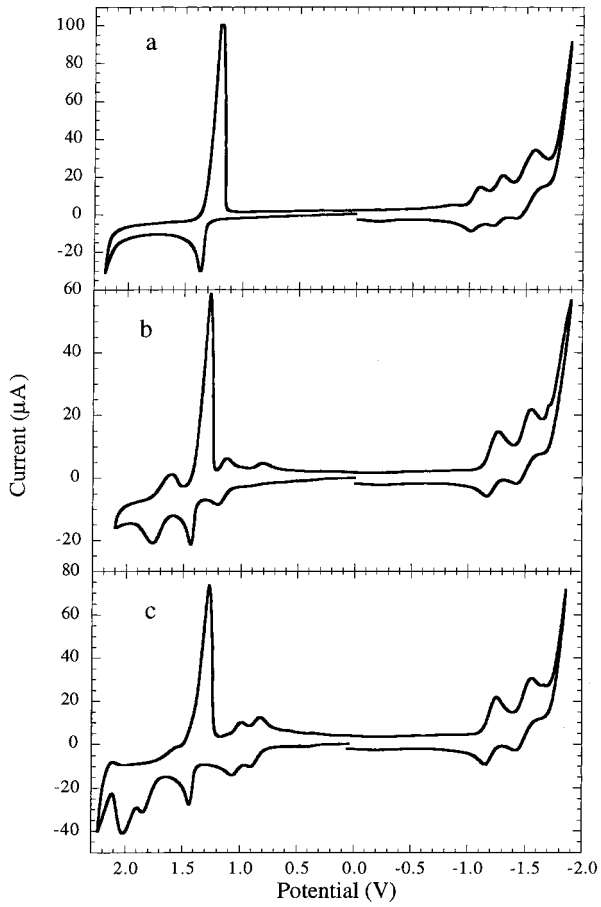

Figure 2. Cyclic voltammograms in dichloromethane for (a) complex **10**, (b) complex **11**, and (c) complex **12**.

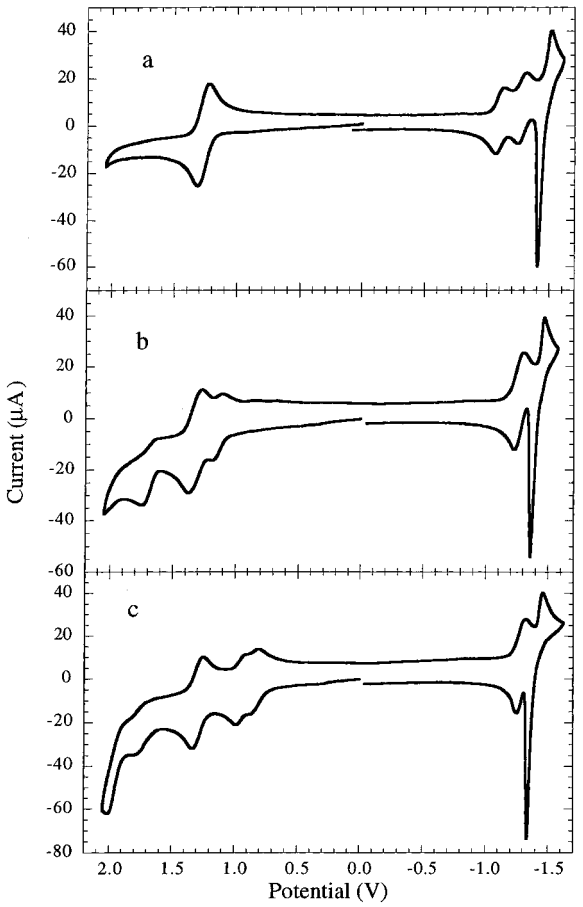

Figure 3. Cyclic voltammograms in acetonitrile for (a) complex **10**, (b) complex **11**, and (c) complex **12**.

employed. Thus, we are forced to conclude that the free-ligand oxidation (at 1.76 V) is dramatically shifted to higher potentials as a result of complexation and by the increased charge generated from the two ruthenium-based oxidations that occur before the oxidation of the bridge.

The cyclic voltammogram of the terthiophene-bridged complex **11** in acetonitrile is shown in Figure 3b. The complex displays three distinct oxidation processes. The first process with $E^{\circ\prime} = 1.15$ V and $n = 1$ is assigned to the oxidation of the terthiophene bridge at slightly more positive potentials with respect to its position in the free ligand. By analogy with complex **10**, the second process at $E^{\circ\prime} = 1.33$ V with $n = 2$ is again assigned to the concurrent oxidation of both Ru(II/III) redox couples. In this case, the ruthenium oxidation is slightly positive relative to the single-thiophene-bridged complex **10** most likely due to the increased positive charge created by the first oxidation process. The third process in complex **10** at $E_{pa} = 1.73$ V with $n = 1$ is assigned to the formation of the dicationic form of the terthiophene bridge, which is not stable on the CV time scale. Contrary to the first terthiophene oxidation process that is not shifted much relative to the free ligand, this process displays a significant shift to more positive potentials with respect to the free ligand. As in the case of the ligand oxidation in complex **10**, the additional positive charges created by the oxidation of the ruthenium centers are the likely cause for the shift to more positive potentials.

Complex **12** gives the most interesting oxidation chemistry of the three complexes studied. The cyclic voltammogram of the sexithiophene-bridged complex **12** in acetonitrile (Figure 3c) displays five distinct oxidation processes. The first two processes at $E^{\circ\prime} = 0.87$ and 0.99 V are sequential $n = 1$ oxidations of the sexithiophene bridge to the radical cation and dication, respectively. As observed for complex **11**, these oxidations that occur before the oxidation of the metals occur at only slighly more positive potentials than those observed in the free ligand. The third process observed for complex **12** at $E^{\circ\prime} = 1.33$ V with $n = 2$ is again assigned to the Ru(II/III) redox couple of the two metal centers. Again, the prior oxidation of the sexithiophene bridging unit produces a slight positive shift on the ruthenium oxidations from the $Ru(bpy)_3^{2+}$ value. In this case, the ruthenium potential is more positive than that in the single-thiophene-bridged complex **10** and is identical to that in complex **11**. The fourth and fifth oxidation processes observed (both with $n = 1$) at $E^{\circ\prime} = 1.79$ V and $E_{pa} = 1.99$ V are assigned to the formation of the trication radical and tetracation of the sexithiophene bridge. The fifth process does not appear to generate a species that is stable on the CV time scale.

In addition to the extensive oxidation chemistry we have observed for the binuclear ruthenium complexes, significant reduction processes are also observed (see Figure 2). The reduction processes of complexes **11** and **12** in dichloromethane are nearly identical (Figure 2b,c). These complexes exhibit three two-electron reduction processes at ca. $E^{\circ\prime} = -1.2$, -1.5, and -1.8 V. The last reduction process is near the solvent/electrolyte limit and could be resolved in the square wave experiment. The most negative two-reduction processes of complexes **11** and **12** occur at nearly the same potential as those of the analogous $n = 1$ processes in $Ru(bpy)_3^{2+}$. These two processes are assigned to concurrent reductions of the ancillary bipyridine ligands at both ruthenium centers. The first reduction processes in

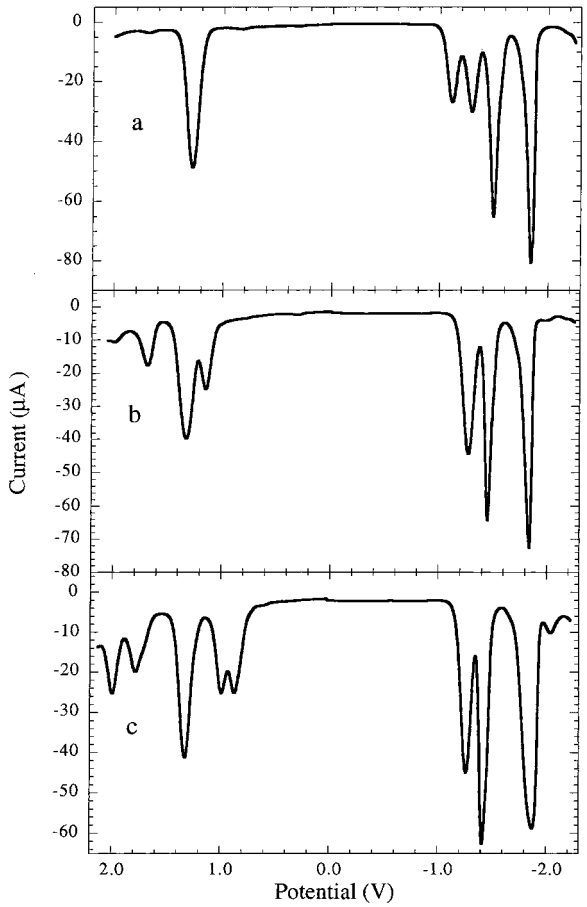

Figure 4. Osteryoung square wave voltammograms in acetonitrile for (a) complex **10**, (b) complex **11**, and (c) complex **12**.

complexes **11** and **12** at −1.27 V in acetonitrile are significantly shifted relative to the first bipyridine reduction in $Ru(bpy)_3^{2+}$ (at 1.31 V) and relative to the first reductions in complex **10** (vide infra). The first reduction processes in complexes **11** and **12** are assigned to concurrent reductions of the bipyridine capping groups of the bridging ligand. Interactions of the oligothiophene bridges with the bipyridine caps shift the bipyridine reductions to less negative values but result in little communication between the bipyridine caps.

The reduction of complex **10** with the shortest bridge in dichloromethane is shown in Figure 2a. Complex **10** exhibits four reduction processes at $E^{\circ\prime} = -1.05$, -1.26, -1.51, and -1.79 V. Again, the final reduction process was resolved in the square wave experiment. As in the case of complexes **11** and **12**, the last two reduction processes involve two electrons each and they occur at potentials nearly identical to those of the analogous one-electron processes in $Ru(bpy)_3^{2+}$. We assign each of these reduction processes to the concurrent reduction of an ancillary bipyridine ligand at each metal center.

Each of the first two processes observed for complex **10** involves one electron and is assigned to the *sequential* reduction of the bipyridine capping units of the bridging ligand. In contrast to the results for complexes **11** and **12**, the addition of the first electron to the bridging ligand and the short bridging distance provided by the single-thiophene ring bridge result in different reduction potentials for the bridging ligand reduction processes.

Conclusions

Changing the number of thiophene rings in the series of oligothiophene bridging ligands $bpy(th)_x bpy$ and their binuclear ruthenium(II) complexes allows the electronic spectroscopy and redox chemistry of the bridge to be adjusted relative to the metal complex caps. For complex **10** with one thiophene ring in the bridge, both ruthenium centers are oxidized at the same potential before the bridge oxidizes. No oxidation of the thiophene ring is observed in this case. The first reductions in **10** occur at the bipyridine caps of the bridging ligand at discrete potentials, followed by concurrent reductions of the ancillary bpy ligands. Complex **11** has concurrent ruthenium oxidations sandwiched between two sequential terthiophene oxidations; complex **12** has the concurrent ruthenium oxidations after two sequential sexithiophene oxidations and before two others. Both **11** and **12** show concurrent reductions at both rutheniums first starting with the bipyridine caps of the bridging ligands followed by the ancillary bpy ligands.

Changes in the electronic structure of the complexes are also apparent in the spectra, but the precise natures of the lowest excited states in **10**, **11**, and **12** are not so obvious. It is clear that the π^* level of the bpy capping group is somewhat lower than the analogous π^* level in the ancillary ligands. This argues for the excited electron of the lowest MLCT state in complexes **11** and **12** to be localized on the capping bpy. The electrochemical results suggest that delocalization in these MLCT states of the excited electron from one ruthenium complex across the bridge to the other complex is not significant. The thermodynamic splitting observed for the reductions in complex **10** suggests that the lowest MLCT state in this binuclear complex could have a significant amount of delocalization of the excited electron across the bridge onto the opposite bipyridine cap. This delocalized structure would result in a significantly higher degree of charge separation in this MLCT state. Unfortunately, a clear assignment of the lowest-lying excited state in **10**, **11**, and **12** to a MLCT state cannot be made because of the close proximity and similar shift behavior of the lowest $\pi-\pi^*$ transition of the oligothiophene bridge. Of the three complexes, it is most likely that complex **10** has a MLCT state that is lowest in energy and contains significant intercomplex charge-transfer character. In addition to the spectroscopically observed states discussed here, rapid electron-transfer reactions of the MLCT or $\pi-\pi^*$ ligand state could produce additional low-energy, charge-separated excited states with oxidized oligothiophene groups and reduced bipyridine ligands. We plan to perform additional experiments (synthesis of the osmium analogues and spectroelectrochemistry, emission lifetime, emission quantum yield, and transient absorption studies) to resolve these issues.

Acknowledgment. This research was supported by the National Science Foundation under Grant CHE-9307837. We thank Jonathan Raff for the synthesis of compound **4**.

IC010549E